ACS Catalysis

Research Article

pubs.acs.org/acscatalysis

Platinum-Coated Cobalt Nanowires as Oxygen Reduction Reaction Electrocatalysts

Shaun M. Alia,[†] Svitlana Pylypenko,[‡] K. C. Neyerlin,[†] David A. Cullen,[§] Shyam S. Kocha,[†] and Bryan S. Pivovar*,[†]

[†]Chemical and Materials Science Center, National Renewable Energy Laboratory, Golden, Colorado 80401, United States

[‡]Department of Metallurgical and Materials Engineering, Colorado School of Mines, Golden, Colorado 80401, United States

[§]Materials Science and Technology Division, Oak Ridge National Laboratory, Oak Ridge, Tennessee 37831, United States

Supporting Information

ABSTRACT: Cobalt nanowires (CoNWs) are coated with platinum (Pt) by partial galvanic displacement, forming core/shell wires 200−300 nm in diameter and 100−200 μm in length. Pt-coated CoNWs (PtCoNWs) are characterized for activity in the oxygen reduction reaction (ORR) with rotating disk electrode half-cells in 0.1 M perchloric acid electrolytes. The resulting catalysts demonstrate ORR-specific activities in the range 2053−2783 μA cm_{Pt}^{-2}, comparable to the specific activity of polycrystalline Pt. The specific activities of PtCoNWs increase with decreasing Pt content and exhibit a corresponding increase in Pt lattice compression. PtCoNWs have exhibited a maximum mass activity of 793 mA mg_{Pt}^{-1}, 2.6 times greater than carbon-supported Pt nanoparticles.

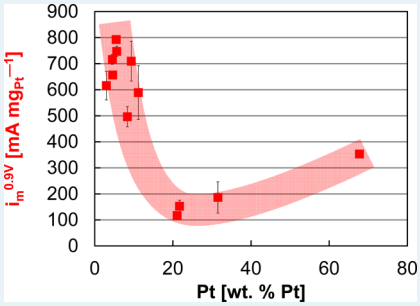

KEYWORDS: *oxygen reduction reaction, fuel cells, electrochemistry, galvanic displacement, extended surfaces*

INTRODUCTION

Platinum (Pt) catalyst cost is one of the barriers to the commercial deployment of proton-exchange membrane fuel cells (PEMFCs).[1] Pt nanoparticles supported on high-surface-area carbon (Pt/HSC) are typically used as PEMFC catalysts. Although Pt/HSC has a high surface area and reasonably high mass activity for the oxygen reduction reaction (ORR), a reduction in catalyst cost is needed to achieve cost targets and to improve the commercial competitiveness of PEMFCs. To provide a guideline in ORR catalyst development, the U.S. Department of Energy (DOE) set an out-year target (2017−2020) of 440 mA mg_{PGM}^{-1} on a Pt group metal (PGM) basis for ORR mass activity in PEMFCs for transportation use. Pt/HSC has an activity that is roughly half that of the target activity; an improvement of catalyst activity by a factor of 4 will allow for the use of <0.1 g kW^{-1} (10 g per 100 kW stack). These loadings will be comparable to the amount of catalyst currently used in ultraclean catalytic converters and mitigate any concern about Pt availability and cost. The DOE target referenced here is a target value for membrane electrode assemblies (MEAs). Throughout the manuscript, we report values obtained from rotating disk electrode (RDE) experiments often making comparisons to DOE MEA targets. The RDE measurements are less susceptible to performance loss factors such as mass transfer and electronic/ionic resistance but can be obtained with smaller sample sizes and less electrode optimization than would be required for MEA tests. RDE performance is a common metric for catalyst screening; direct comparisons with MEA performance, such as those presented in this manuscript, can be useful as a qualitative screen but do not guarantee similar performance within MEAs. Pt/HSC durability is also a concern and is limited by degradation of the carbon support and Pt loss due to Ostwald ripening, potential-driven dissolution, and aggregation due to surface tension.[2−4]

Studies were previously completed investigating Pt cobalt (Co) films and nanomaterials for ORR activity. Nørskov et al. and Stamenković et al. studied polycrystalline Pt films alloyed with a variety of transition metals; Pt_3Co was found to be the most active of those examined, with a specific activity 3−4 times greater than Pt.[5,6] The work of Strasser et al. and Paulus et al. continued into nanoparticle catalysts, finding PtCo alloys with specific activities 3 times greater than carbon-supported Pt nanoparticles.[7,8] Shao-Horn et al. similarly studied Pt_3Co nanoparticles that produced 80% the DOE target for mass activity in ORR.[9] Chen et al. further examined Pt Co nanowires, synthesized by a microwave-assisted coreduction process.[10] The mass ORR activity of the Pt Co nanowires, however, did not meet that of carbon-supported Pt. Nanostructured thin-film (NSTF) catalysts have been developed by 3M, demonstrating significant improvements in specific ORR activity compared with Pt nanoparticles.[11] These catalysts were then alloyed with Co and manganese (Mn), further increasing the specific activity about 3 times (about 10 times compared with Pt nanoparticles).[12] Although the surface area of these materials is low, the high specific activity allows for PtCoMn

Received: March 20, 2014
Revised: June 26, 2014
Published: July 3, 2014

NSTF to approach the DOE mass activity target (~350 mA mg_{PGM}^{-1} at 60 °C) in RDE half-cells.

Extended surface Pt structures have been studied previously for ORR activity and have demonstrated specific activity and durability benefits compared with Pt nanoparticles.[11−14] Although extended surfaces reduced the number of low coordination sites and improved specific activity, the surface areas have generally been low and unable to meet the DOE mass activity target or to ensure the commercial deployment of PEMFCs. Subsequent efforts in developing extended surface Pt catalysts have focused on improving surface area by introducing porosity, employing alternative morphologies, or "thrifting" the Pt content by partial displacement using palladium, copper, and nickel (Ni) as substrate materials.[15−20]

Co nanowires (CoNWs) were used as the template material in this study in an effort to improve both Pt utilization and specific ORR activity. The use of CoNWs potentially improves ORR specific activity by employing an extended surface with the potential benefits associated with Co alloying.[21,22] Partial galvanic displacement also potentially allows for the formation of a thin Pt layer, improving the Pt-normalized surface area. Co has the additional benefit of a negative standard redox potential (−0.28 V vs a reversible hydrogen electrode, RHE) and was chosen to avoid template metals that could migrate through the membrane and plate on the anode during typical PEMFC operation. This study has strong parallels with other work from our team using Ni nanowires (NiNWs) as templates.[20] Throughout this paper, we will compare the results of this study to those obtained using NiNWs. This study has benefitted from collaborations with the research groups of Yushan Yan at the University of Delaware and University of California, Riverside.[18,19]

EXPERIMENTAL

CoNWs (40 mg, PlasmaChem GmbH) were dispersed by horn sonication (2 min) in 80 mL of deionized water. The CoNW dispersion was heated to 90 °C in an oil bath and stirred at about 400 rpm with a Teflon paddle connected by a glass rod to a rotator. Partial spontaneous galvanic displacement was completed by adding varying amounts of potassium tetrachloroplatinate to the CoNWs (Supporting Information (SI) Figure S1). The potassium tetrachloroplatinate was added to 15 mL of deionized water and added dropwise over 15 min to the CoNW dispersion.

Inductively coupled plasma mass spectrometry (ICP-MS) experiments were completed using a Thermo Scientific iCAP Q. Pt-coated CoNWs (PtCoNWs) were weighed with a microbalance and digested in aqua regia. Samples were diluted to three concentrations (aimed at 2, 20, 100 ppb Pt) using energy-dispersive X-ray spectroscopy (EDS) measurements in field-emission scanning electron microscopy (FESEM) experiments as a guide. ICP-MS measurements were taken with three standards and a blank, with an internal standard taken every five unknowns. Measurements of each unknown included a full-spectrum screening and three measurements taken with dwell times of 0.05 s. Standard deviations among these measurements were less than 2% of the average concentration. Catalyst compositions were calculated using the Pt-to-Co concentration ratio, assuming that the samples contained only Pt and Co. Oxide content was not accounted for in ICP-MS measurements. The Pt content therefore contained a systematic error and was slightly overestimated. Electrochemical values that were normalized to Pt loading (surface area, ORR mass activity) were therefore slightly underestimated.

Synchrotron-based X-ray diffraction (XRD) experiments were conducted at the Stanford Synchrotron Radiation Lightsource (Stanford Linear Accelerator Center), beamline 2-1 using X-ray energy at 11.4 keV. Samples were prepared for XRD by pipetting samples (dispersed in isopropyl alcohol) onto carbon tape adhesive and allowing them to dry.

FESEM and EDS analysis were performed using a JEOL JSM-7000F field emission microscope equipped with an EDAX Genesis energy dispersive X-ray spectrometer. Transmission electron microscopy (TEM) micrographs were obtained on a Philips CM200 transmission electron microscope equipped with a Princeton Gamma-Tech Prism energy dispersive X-ray spectrometer. PtCoNWs subjected to electrochemical break-in and durability testing were prepared by sonicating the RDE tip in isopropyl alcohol (~1 mL). X-ray photoelectron spectroscopy (XPS) was completed on a Kratos Nova X-ray photoelectron spectrometer equipped with a monochromatic Al Kα source operated at 300 W. Nonconductive adhesive was used to mount samples for analysis. Spectra were acquired at pass energies of 160 and 20 eV for survey and high-resolution spectra, respectively, while providing charge compensation using low energy electrons. CasaXPS software was used for data analysis and data processing included background subtraction (linear for C 1s and O 1s, Shirley for Ni 2p and Pt 4f).

Thin cross sections of PtCoNWs were prepared by diamond-knife ultramicrotomy. The nanowires were mounted in epoxy, then cut into 50 nm sections and mounted on 3 mm copper grids. The cross-sections were then studied by scanning transmission electron microscopy (STEM) and EDS spectrum imaging in an aberration-corrrected JEOL JEM2200-FS. Spectrum images were recorded using a Bruker XFlash silicon drift detector.

Electrochemical experiments were completed in a RDE half-cell filled with a 0.1 M perchloric acid electrolyte. The RDE cell was equipped with a glassy carbon working electrode, a Pt mesh counter electrode, and a Pt wire reference electrode.[23,24] The Pt wire reference electrode was contained in a separate compartment saturated with hydrogen and was connected to the main cell by a luggin capillary. Rotation of the working electrode was controlled by a modulated speed rotator (Pine Instrument Company), and electrochemical measurements were taken with a single-channel Autolab potentiostat (Eco Chemie, Metrohm Autolab B.V.).

PtCoNW inks were prepared at a concentration of 0.15−0.20 mg_{PtCo} mL^{-1} for 5 mL of total ink containing 3.8 mL of deionized water, 1.2 mL of isopropyl alcohol, and 20 μL of Nafion ionomer.[25,26] The PtCoNW inks were used with relatively dilute Pt Co concentrations to prevent catalyst agglomeration during the coating process. Inks were sonicated in ice by the following regimen: 30 s horn sonication; 30 min bath sonication; 30 s horn sonication; 10 min bath sonication; and 30 s horn sonication. After sonication, 10 μL of the ink was pipetted onto the glassy carbon working electrode and dried for 20 min at 40 °C. To ensure that ORR experiments reached a full diffusion-limited current, working electrodes were coated with additional aliquots of ink (SI Figure S2). Inks were continually sonicated in ice during this process (20 min bath sonication, 30 s horn sonication, pipet 10 μL), and the electrode loadings were increased to 30−40 μg_{PtCo} cm_{elec}^{-2}. Inks were subsequently added to graphitized carbon nanofibers

dx.doi.org/10.1021/cs500370q | ACS Catal. 2014, 4, 2680−2686

(60 wt %) to improve ink dispersion, and the coating process was repeated on polished glassy carbon working electrodes.[26]

Pt/HSC (46 wt % Pt, Tanaka Kikinzoku Kogyo) was used as a benchmark catalyst in this study, with electrodes coated to 17.8 μg_{Pt} cm^{-2}. Pt/HSC inks contained 7.6 mg of catalyst, 7.6 mL of deionized water, 2.4 mL of isopropyl alcohol, and 40 μL of Nafion ionomer. The inks were bath-sonicated for 20 min prior to dispensing 10 μL of ink onto the electrode surface (dried 20 min at 40 °C).

The electrochemical surface areas (ECAs) of catalysts were measured during cyclic voltammograms in the range of hydrogen adsorption onto the Pt surface, assuming a Coulombic charge of 210 $\mu C\ cm_{Pt}^{-2}$.[27] Cyclic voltammograms were taken on PtCoNWs in the potential window of 0.025−1.4 V at 100 mV s^{-1} and on Pt/HSC in the potential window of 0.025−1.0 V at 20 mV s^{-1}. ORR data were taken during anodic potential sweeps (−0.01−1.00 V vs RHE) in an oxygen-saturated electrolyte; ORR activities were corrected for internal resistance (18−25 Ω depending on catalyst, each electrode measured), the partial pressure of oxygen (83.2 kPa at 5674 ft), and mass transport (Koutecky−Levich equation). At elevation (5674 ft), the diffusion-limited currents for ORR (4.2−4.8 mA cm_{elec}^{-2}) are lower than typically obtained at sea level due to the lower partial pressure of oxygen (83.2 kPa). Diffusion-limited currents were not corrected in the potential−current figures, but were corrected in the reported kinetic activities. The diffusion-limited currents, when corrected for the local partial pressure of oxygen (83.2 kPa), correspond to 5.1−5.8 mA cm_{elec}^{-2}, which at a rotation speed of 1600 rpm are within the range of theoretically anticipated values. Kinetic currents (ORR) were corrected for the partial pressure of oxygen by a previously, experimentally determined reaction order (∼0.75 at 0.9 V vs RHE in 0.1 M perchloric acid).[28−30] Durability testing was completed by potential cycling (0.6−1.0 V vs RHE) 30 000 times without rotation in a nitrogen-saturated electrolyte.[31] Full cyclic voltammograms were periodically taken (every 1000 cycles up to 5000 cycles, every 5000 cycles after) to monitor catalyst ECA; ORR data were taken following durability testing.

RESULTS AND DISCUSSION

PtCoNWs were synthesized by the partial spontaneous galvanic displacement of CoNWs with Pt. FESEM (Figure 1) and STEM images (SI Figures S3 and S4) confirmed that PtCoNWs maintained the same morphological dimensions as the purchased CoNWs (200−300 nm in diameter, 100−200 μm in length). TEM images were included (SI Figure S5), along with STEM images to confirm nanowire morphology and microstructure. ICP-MS measurements determined that PtCoNWs 2.1−67.7 wt % Pt were synthesized by exposure of CoNWs to 2.7−172.5 mg potassium tetrachloroplatinate.

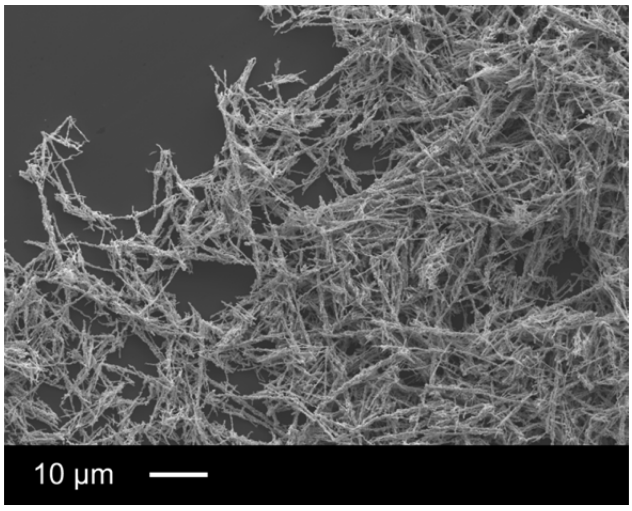

Figure 1. FESEM image of PtCoNWs (5.5 wt % Pt).

At a low displacement level (5.5 wt % Pt), Pt was localized to the surface of the PtCoNWs (Figure 2 and SI Figures S3, S4, S6, and S7). EDS line scans extracted from spectrum images of cross-sectioned PtCoNWs (5.5 wt % Pt) confirmed a Pt response at the outer perimeter of the Co metal template (Figure 2). XPS further found that increasing levels of Pt displacement resulted in increased Pt content near the surface (SI Table S1). High-resolution microscopy (SI Figure S7) was further used to confirm Pt surface features in the 2−4 nm range. In STEM images, a layer of Co oxide appeared separate the outer Pt layer from the metallic Co core (SI Figure S7). A thin oxide layer was present on the CoNWs prior to displacement and small amounts of Co oxide persisted following Pt displacement. The nanowire core remained metallic Co, and the prevalence of Co oxide was small enough to not appear in XRD spectra (Figure 2). These catalysts were therefore referred to as PtCoNWs, without a separate designation made for the thin surface oxide layer. Despite the presence of the Co oxide layer, Pt displacement was found to proceed to 67.7 wt % Pt solely by exposure to potassium tetrachloroplatinate. The degree of displacement is one way in which CoNWs behaved differently from NiNWs, as NiNWs achieved a maximum displacement of 16.4% (wt % Pt) without the addition of acid (hydrochloric).[20]

STEM of cross-sectioned PtCoNWs (5.5 wt % Pt) provided useful morphological and compositional information on the PtCoNWs. These experiments, however, yield two-dimensional renderings of three-dimensional structures and inherently have certain limitations. STEM images were taken on microtomed slices with thicknesses of ∼50 nm. The PtCoNWs were randomly oriented in the epoxy resin, and images reported were taken on samples that were perceived to have the cleanest cross sections (SI Figures S3 and S4). The diameter of the CoNW template varied greatly, with as much as a 50−100 nm diameter change in 50 nm of wire length (SI Figure S6). Overlap in the EDS maps is therefore expected because of imperfect cylindrical morphology and sample orientation. The EDS line scan (Figure 2) reported for a PtCoNW was chosen because of the relative cleanliness of the cross section and the relative narrowness of the Pt region (10−15 nm) of the line scan. Still, this line scan represents an upper bound for the Pt "shell" thickness, and it is expected to be much thinner than this on average (inferred from high-resolution microscopy similar to that reported in SI Figure S7 and from surface-area measurements).

XRD experiments were completed on a range of PtCoNW compositions (5.5−67.7 wt % Pt, Figure 3). In PtCoNWs with clear Co peaks (5.5−31.5 wt % Pt), a bulk Co lattice parameter of 3.55 Å was measured. Similarly, on PtCoNWs (67.7 wt % Pt), a bulk Pt lattice of 3.92 Å was measured; however, on the lower displaced PtCoNWs with clear Pt peaks, the XRD peaks measured were slightly compressed relative to bulk Pt. The Pt lattice further increased in compression with decreasing Pt content. Specifically, PtCoNWs with 31.5, 21.1, and 8.4 wt % Pt

dx.doi.org/10.1021/cs500370q | ACS Catal. 2014, 4, 2680−2686

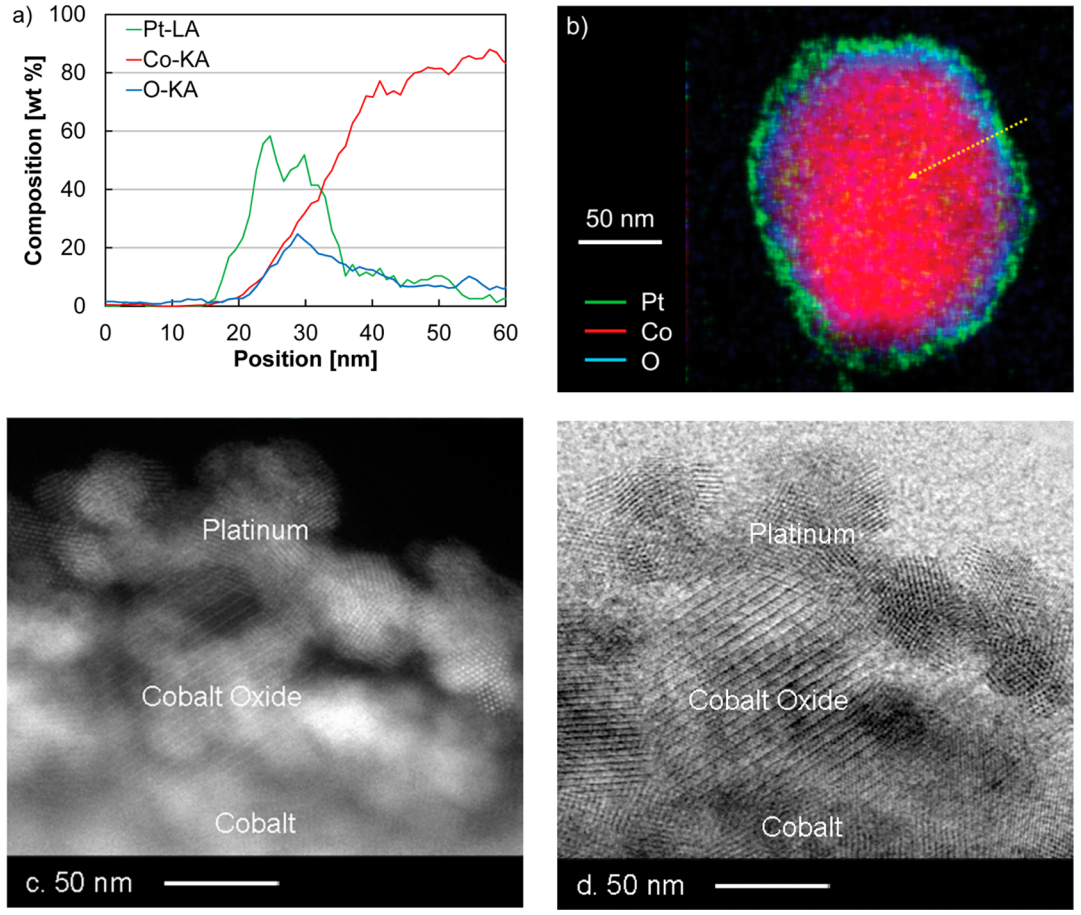

Figure 2. (a) EDS line scan derived from a (b) spectrum image of cross-sectioned PtCoNWs (5.5 wt % Pt) showing the Pt layer, as well an oxide layer between the Pt catalyst and Co nanowire. (c) High-angle annular dark-field and (d) bright-field STEM images of the nanowire surface showing the Co, oxide and Pt layers.

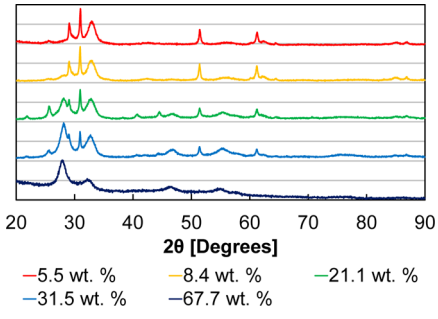

Figure 3. XRD patterns of PtCoNWs containing 5.5, 8.4, 21.1, 31.5, and 67.7 wt % Pt.

were found to have Pt lattice constants of 3.89, 3.88, and 3.87 Å, respectively.

Electrochemical experiments were completed in an RDE half-cell containing a 0.1 M perchloric acid electrolyte. Prior to ECA and ORR determinations, PtCoNWs were potential-cycled to clean the sample of surface Co and to ensure a stable surface. Break-in of the PtCoNWs was performed in the potential range of 0.025−1.4 V vs RHE; the potential cycling continued after sitting overnight in air, immediately prior to testing for ECA and ORR activity. In total, 100−200 cycles were performed on the PtCoNWs during the break-in procedure.

Pt ECAs were calculated during cyclic voltammograms from the charge associated with hydrogen adsorption, assuming a Coulombic charge of 210 μC cm_{Pt}^{-2} (SI Figure S8).[27] The ECA calculation was also performed on a polished polycrystalline Pt electrode; the calculated ECA was 1.2 times greater than the geometric surface, yielding a roughness factor of 1.2 and validating the appropriateness of the calculation. The ECA of PtCoNWs increased with decreasing Pt content. The lower level of displacement appeared to allow more Pt to remain available electrochemically, increasing the ECA relative to the Pt mass. A maximum ECA of 29.1 m^2 g_{Pt}^{-1} was achieved in the PtCoNWs with 5.5 wt % Pt. This ECA, although quite reasonable for an extended-surface catalyst, was significantly lower than that obtained in our previous work for Pt-coated NiNWs (PtNiNWs) at similar displacement levels.[20] In the case of PtNiNWs, ECAs as high as 91.3 m^2 g_{Pt}^{-1} were obtained, about 3 times greater than that of PtCoNWs.

ORR mass and specific activities were determined during anodic polarization scans at 1600 rpm in a 0.1 M perchloric acid electrolyte (Figures 4 and 5). ORR activities were taken at 0.9 V vs RHE and were corrected for internal resistance, the partial pressure of oxygen, and mass transport. PtCoNWs (5.5 wt % Pt) produced a maximum mass activity of 793 mA mg_{Pt}^{-1}, 2.6 times greater than Pt/HSC (306 mA mg_{Pt}^{-1}) and 1.8 times greater than the DOE target. PtCoNWs produced a range of specific activities, from 2783 μA cm_{Pt}^{-2} (4.5 wt % Pt) to 2053 μA cm_{Pt}^{-2} (67.7 wt % Pt). In general, the specific activity of

dx.doi.org/10.1021/cs500370q | ACS Catal. 2014, 4, 2680−2686

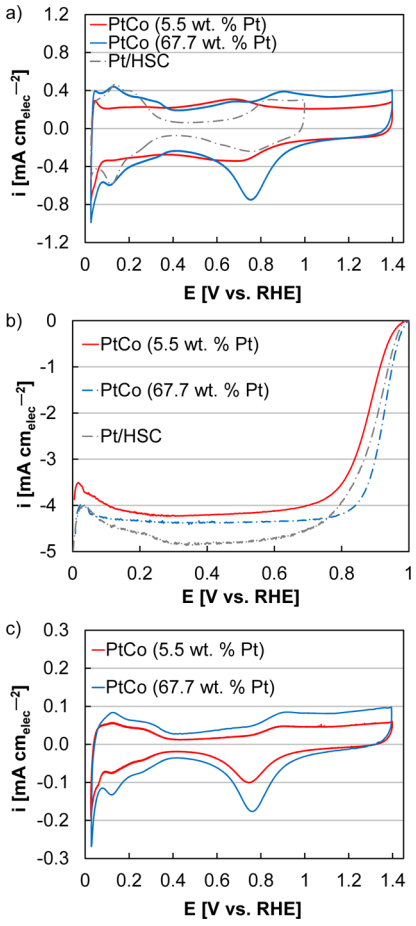

Figure 4. (a) Cyclic voltammograms and (b) ORR polarization curves of PtCoNWs (5.5 and 67.7 wt % Pt with graphitized carbon nanofibers, 60 wt %, added to catalyst inks) and Pt/HSC. (c) Cyclic voltammograms of PtCoNWs (5.5 and 67.7 wt % Pt without graphitized carbon nanofibers added). Catalyst loadings on the RDE tip were as follows: PtCoNWs (5.5 wt % Pt) 30.6 μg_{PtCo} cm_{elec}^{-2}; PtCoNWs (67.7 wt %) 40.4 μg_{PtCo} cm_{elec}^{-2}; and Pt/HSC 17.8 μg_{Pt} cm_{elec}^{-2}. The diffusion-limited currents of the ORR polarization curves are lower than observed at sea level due to the partial pressure of oxygen at elevation (83.2 kPa); more information is available in the Experimental section.

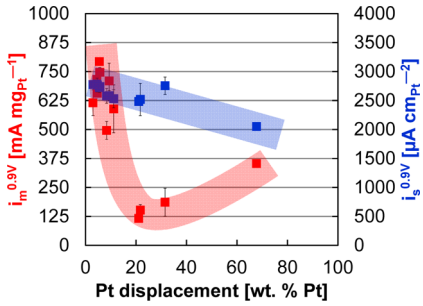

Figure 5. Mass and specific ORR activities of PtCoNWs as a function of percent Pt displacement. ORR measurements were taken during anodic polarization scans (1600 rpm, 20 mV s^{-1}) in an oxygen-saturated 0.1 M perchloric acid electrolyte and were corrected for internal resistance, the partial pressure of oxygen, and mass transport. PtCoNW inks in these measurements contained 60 wt % graphitized carbon nanofibers.

PtCoNWs decreased with increasing Pt content. The highest PtCoNW specific activity (2783 $\mu A\ cm_{Pt}^{-2}$ at 4.5 wt % Pt) was greater than Pt/HSC (304 $\mu A\ cm_{Pt}^{-2}$) by 9.2 times and polycrystalline Pt (2245 $\mu A\ cm_{Pt}^{-2}$) by 1.2 times. The specific activities of the PtCoNWs were significantly higher than those obtained for PtNiNWs.[20] Because of this, the peak mass activity of PtCoNWs (793 mA mg_{Pt}^{-1}) approached the peak value obtained for PtNiNWs (917 mA mg_{Pt}^{-1}) but remained slightly inferior.

PtCoNW inks were prepared with relatively dilute concentrations of Pt and Co (0.15–0.20 $mg_{PtCo}\ mL^{-1}$) to prevent catalyst agglomeration during the electrode-coating process. Graphitized carbon nanofibers (60 wt %) were also added to the inks to aid in catalyst dispersion. The use of carbon nanofibers marginally improved surface area (up to 10%, SI Figures S8 and S9) and consistently improved mass and specific activity for ORR (10–20%, SI Figure S10).

Durability testing was conducted on PtCoNWs and Pt/HSC by potential cycling (30 000 cycles, 0.6–1.0 V vs RHE) in RDE half-cells. Full cyclic voltammograms were taken periodically to monitor the ECAs of the catalysts (SI Figure S11). On a percentage basis, the degree of ECA loss in PtCoNWs was generally comparable to Pt/HSC. Although extended Pt structures were previously found to maintain a higher proportion of ECA in potential cycling, Co is susceptible to dissolution, potentially reducing durability benefits. TEM images were taken of PtCoNWs (21.1 wt % Pt, as determined by ICP-MS) prior to electrochemical testing, following electrochemical break-in, and following durability testing (Figure 6). EDS measurements taken on the as-synthesized

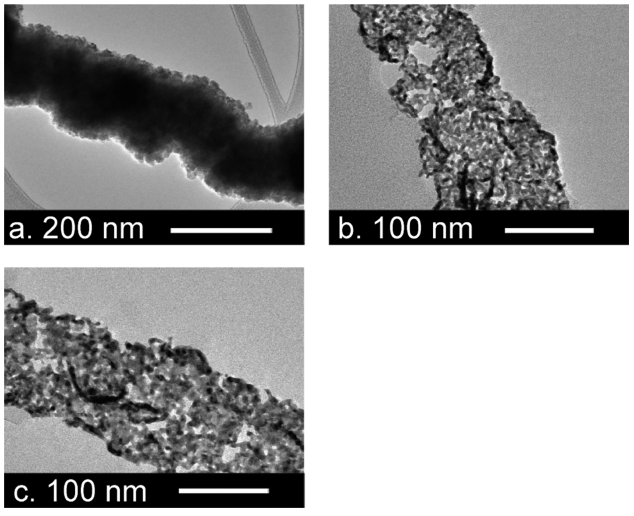

Figure 6. TEM images of PtCoNWs (21.1 wt % Pt): (a) as-synthesized, (b) following electrochemical break-in, and (c) following durability testing.

sample found 75 wt % Co. In electrochemical break-in, Co apparently leached from the PtCoNWs to 5 wt % Co (as determined by EDS measurements). Although PtCoNWs routinely lost 20% ECA in durability testing, the Co content largely remained the same (5 wt % Co, as determined by EDS measurements). The TEM image following electrochemical break-in also partially speaks to the continuity of the Pt layer at a moderate level of Pt displacement. Once the majority of Co was removed, the deposited porous Pt layer maintained the original outer morphological dimensions of the as-synthesized

dx.doi.org/10.1021/cs500370q | ACS Catal. 2014, 4, 2680–2686

PtCoNWs but also clearly showed voids in the Pt "shell" structure. These results are in stark contrast to results obtained for PtNiNWs, where exposure to acid and break-in/durability cycling was found to have essentially no impact on catalyst structure, even though this system was investigated at a much lower Pt displacement (9.6 wt % Pt) level.[20]

Following durability testing, ORR measurements were again taken on PtCoNWs and Pt/HSC (Figure 7 and SI Figures S12 and S13). The specific ORR activities and the ECAs of PtCoNWs each decreased 10−20% following potential cycling. Nonetheless, several of the PtCoNW samples maintained ORR mass activities that exceeded the DOE target. The highest PtCoNW performer (4.5 wt % Pt) following potential cycling produced an ORR mass activity of 579 mA mg_{Pt}^{-1}. In comparison, Pt/HSC produced an ORR mass activity of 225 mA mg_{Pt}^{-1} following durability testing.

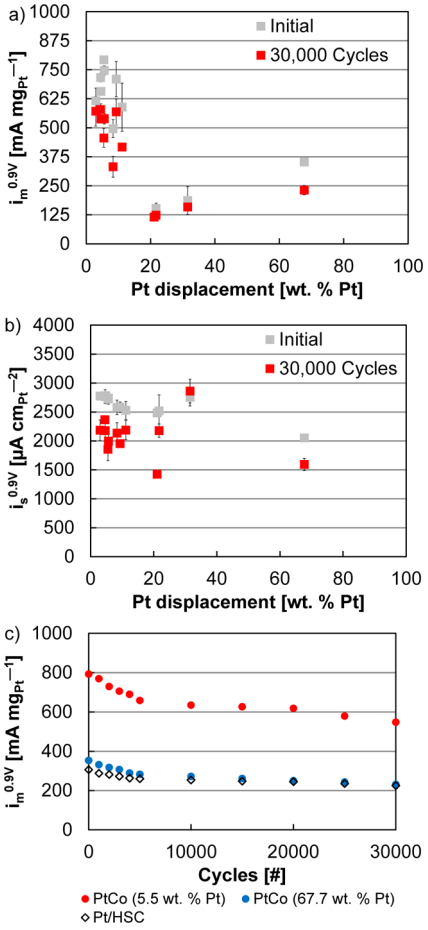

Figure 7. (a) Mass and (b) specific ORR activities of PtCoNWs as a function of percent Pt displacement prior to and following durability testing. Durability testing was completed by potential cycling (30 000 cycles, 0.6−1.0 V vs RHE) in a nitrogen-saturated 0.1 M perchloric acid electrolyte. (c) Mass ORR activities of PtCoNWs (5.5 and 67.7 wt % Pt) and Pt/HSC as a function of durability cycle. Durability testing was completed by potential cycling (30 000 cycles, 0.6−1.0 V vs RHE) in an oxygen-saturated 0.1 M perchloric acid electrolyte. ORR measurements were taken during anodic polarizations (1600 rpm, 20 mV s^{-1}) in an oxygen-saturated 0.1 M perchloric acid electrolyte and were corrected for internal resistance, the partial pressure of oxygen, and mass transport. PtCoNW inks in these measurements contained 60 wt % graphitized carbon nanofibers.

The extended surface and electronic structure of Pt have previously been cited in explaining the activity of similar Pt catalysts.[11,22] Extended-surface Pt catalysts have previously been found to have higher specific activity for ORR, partially attributed to reducing low-coordination edge sites.[11,13,21] Although Pt displacement of CoNWs formed a Pt layer with nanoparticle surface features, the PtCoNWs appeared to benefit from the extended surface nature of the catalyst, producing ORR specific activities on a level comparable to polycrystalline Pt. The electronic structure of Pt was also potentially modified by a Co alloying effect and by the elimination of Pt-C interaction.[21,22] The use of the CoNW template resulted in a compressed Pt lattice (at low levels of displacement); the Co alloying effect potentially improved ORR activity by electronically tuning Pt, influencing the band structure, and decreasing the strength of Pt−O binding on the surface.[22]

This study roughly paralleled another our group completed on PtNiNWs.[20] Significant differences were observed between the two templates. High levels of displacement were achieved using CoNWs (up to 67.7 wt % Pt), whereas the displacement of NiNWs was limited to 16.4 wt % Pt (without the addition of hydrochloric acid).[20] An oxide layer (present in both CoNWs and NiNWs) appeared to have a larger role in the case of NiNWs. The use of CoNWs also allows for Pt lattice compression (at low displacement) not seen with the NiNWs. PtCoNWs and PtNiNWs produced similar ORR mass activities but achieved these activities in different ways (Table 1). For the highest-performing catalysts (maximum mass activity), the specific activities of PtCoNWs (2725 μA cm_{Pt}^{-2}) were higher than PtNiNWs (1295 μA cm_{Pt}^{-2}). Conversely, the ECAs were lower (29.1 m^2 g_{Pt}^{-1} compared to 70.9 m^2 g_{Pt}^{-1}). Future development of these catalysts would ideally utilize the ECAs observed in the PtNiNWs and the specific activities observed in the PtCoNWs, allowing for even further enhancements of mass activity.

Table 1. Comparison of PtCoNWs and PtNiNWs, High Performers[a].

	ECA, m^2 g_{Pt}^{-1}	$i_m^{0.9V}$, mA mg_{Pt}^{-1}	$i_s^{0.9V}$, μA cm_{Pt}^{-2}
PtCoNW	29.1	793	2725
PtNiNW	70.9	917	1295

[a]Initial activity.

CONCLUSIONS

PtCoNWs were studied as ORR catalysts in RDE half-cells and were found to have high specific and mass activities for ORR and beneficial durability characteristics. As the Pt content was decreased, the specific ORR activity increased from 2053 μA cm_{Pt}^{-2} (67.7 wt % Pt) to as high as 2783 μA cm_{Pt}^{-2} (4.5 wt % Pt), exceeding polycrystalline Pt (1.2 times the activity). ECA also increased with decreasing Pt content, to a high of 29.1 m^2 g_{Pt}^{-1} (5.5 wt % Pt). PtCoNWs (5.5 wt % Pt) were thereby able to produce a peak mass ORR activity 2.6 times greater than Pt/HSC and 1.8 times greater than the DOE target for ORR activity in PEMFCs. PtCoNWs also retained a high level of ORR activity following potential cycling. Of the 10 catalysts that exceeded the DOE target for ORR, 8 still exceeded the target following durability testing. PtCoNWs (4.5 wt % Pt) produced a peak ORR activity 1.3 times greater than the DOE target after potential cycling. Through this study, the potential

dx.doi.org/10.1021/cs500370q | ACS Catal. 2014, 4, 2680−2686

benefit of PtCoNWs as ORR catalysts in PEMFCs was demonstrated.

■ ASSOCIATED CONTENT

Supporting Information

Additional figures. This material is available free of charge via the Internet at http://pubs.acs.org.

■ AUTHOR INFORMATION

Corresponding Author

*Fax: (303) 275-3840. E-mail: bryan.pivovar@nrel.gov.

Notes

The authors declare no competing financial interest.

■ ACKNOWLEDGMENTS

Financial support is provided by the U.S. Department of Energy, Office of Energy Efficiency and Renewable Energy, by Contract No. DE-AC36-08GO28308.

■ REFERENCES

(1) Gasteiger, H.; Kocha, S.; Sompalli, B.; Wagner, F. *Appl. Catal., B* **2005**, *56*, 9−35.

(2) Borup, R.; Meyers, J.; Pivovar, B.; Kim, Y.; Mukundan, R.; Garland, N.; Myers, D.; Wilson, M.; Garzon, F.; Wood, D.; Zelenay, P.; More, K.; Stroh, K.; Zawodzinski, T.; Boncella, J.; McGrath, J.; Inaba, M.; Miyatake, K.; Hori, M.; Ota, K.; Ogumi, Z.; Miyata, S.; Nishikata, A.; Siroma, Z.; Uchimoto, Y.; Yasuda, K.; Kimijima, K.; Iwashita, N. *Chem. Rev.* **2007**, *107*, 3904−3951.

(3) Darling, R.; Meyers, J. *J. Electrochem. Soc.* **2003**, *150*, A1523−A1527.

(4) Ferreira, P.; la O', G.; Shao-Horn, Y.; Morgan, D.; Makharia, R.; Kocha, S.; Gasteiger, H. *J. Electrochem. Soc.* **2005**, *152*, A2256−A2271.

(5) Stamenkovic, V.; Mun, B.; Mayrhofer, K.; Ross, P.; Markovic, N.; Rossmeisl, J.; Greeley, J.; Nørskov, J. *Angew. Chem.* **2006**, *118*, 2963−2967.

(6) Stamenković, V.; Schmidt, T.; Ross, P.; Marković, N. *J. Phys. Chem. B* **2002**, *106*, 11970−11979.

(7) Paulus, U.; Wokaun, A.; Scherer, G.; Schmidt, T.; Stamenkovic, V.; Radmilovic, V.; Markovic, N.; Ross, P. *J. Phys. Chem. B* **2002**, *106*, 4181−4191.

(8) Koh, S.; Leisch, J.; Toney, M. F.; Strasser, P. *J. Phys. Chem. C* **2007**, *111*, 3744−3752.

(9) Chen, S.; Sheng, W.; Yabuuchi, N.; Ferreira, P. J.; Allard, L. F.; Shao-Horn, Y. *J. Phys. Chem. C* **2008**, *113*, 1109−1125.

(10) Higgins, D. C.; Ye, S.; Knights, S.; Chen, Z. *Electrochem. Solid-State Lett.* **2012**, *15*, B83−B85.

(11) Debe, M., Ed.; U.S. Department of Energy: Washington, D.C., 2008; http://www.hydrogen.energy.gov/pdfs/review08/fc_1_debe.pdf.

(12) Debe, M., Ed.; U.S. Department of Energy, Washington, D.C., 2009; http://www.hydrogen.energy.gov/pdfs/review09/fc_17_debe.pdf.

(13) Chen, Z.; Waje, M.; Li, W.; Yan, Y. *Angew. Chem., Int. Ed.* **2007**, *46*, 4060−4063.

(14) Papandrew, A. B.; Atkinson, R. W.; Goenaga, G. A.; Wilson, D. L.; Kocha, S. S.; Neyerlin, K. C.; Zack, J. W.; Pivovar, B. S.; Zawodzinski, T. A. *ECS Trans.* **2013**, *50*, 1397−1403.

(15) Alia, S.; Zhang, G.; Kisailus, D.; Li, D.; Gu, S.; Jensen, K.; Yan, Y. *Adv. Funct. Mater.* **2010**, *20*, 3742−3746.

(16) Larsen, B.; Neyerlin, K.; Bult, J.; Bochert, C.; Blackburn, J.; Kocha, S.; Pivovar, B. *J. Electrochem. Soc.* **2012**, *159*, F622−F627.

(17) Alia, S.; Jensen, K.; Pivovar, B.; Yan, Y. *ACS Catal.* **2012**, *2*, 858−863.

(18) Alia, S.; Jensen, K.; Contreras, C.; Garzon, F.; Pivovar, B.; Yan, Y. *ACS Catal.* **2013**, *3*, 358−362.

(19) Pivovar, B., Ed.; U.S. Department of Energy: Washington, D.C., 2013; http://www.hydrogen.energy.gov/pdfs/review13/fc007_pivovar_2013_o.pdf.

(20) Alia, S. M.; Larsen, B. A.; Pylypenko, S.; Cullen, D. A.; Diercks, D. R.; Neyerlin, K. C.; Kocha, S. S.; Pivovar, B. S. *ACS Catal.* **2014**, *4*, 1114−1119.

(21) Kinoshita, K. *J. Electrochem. Soc.* **1990**, *137*, 845−848.

(22) Nørskov, J.; Rossmeisl, J.; Logadottir, A.; Lindqvist, L.; Kitchin, J.; Bligaard, T.; Jónsson, H. *J. Phys. Chem. B* **2004**, *108*, 17886−17892.

(23) Takahashi, I.; Kocha, S. *J. Power Sources* **2010**, *195*, 6312−6322.

(24) Garsany, Y.; Baturina, O.; Swider-Lyons, K.; Kocha, S. *Anal. Chem.* **2010**, *82*, 6321−6328.

(25) Kocha, S.; Zack, J.; Alia, S.; Neyerlin, K.; Pivovar, B. *ECS Trans.* **2013**, *50*, 1475−1485.

(26) Neyerlin, K. C.; Larsen, B. A.; Pylypenko, S.; Kocha, S. S.; Pivovar, B. S. *ECS Trans.* **2013**, *50*, 1405−1413.

(27) Biegler, T.; Rand, D.; Woods, R. *J. Electroanal. Chem. Interfacial Electrochem.* **1971**, *29*, 269−277.

(28) Neyerlin, K. C.; Gu, W.; Jorne, J.; Gasteiger, H. A. *J. Electrochem. Soc.* **2006**, *153*, A1955−A1963.

(29) Takahashi, I.; Kocha, S. S. *J. Power Sources* **2010**, *195*, 6312−6322.

(30) Kocha, S. S. In *Handbook of Fuel Cells − Fundamentals, Technology and Applications*; Vielstich, W., Lamm, A., Gasteiger, H. A., Eds.; Wiley: Chichester, New York, 2003; Vol. 3; pp 538−565.

(31) Kocha, S. In *Polymer Electrolyte Fuel Cell Degradation*; Mench, M., Kumbur, E. C., Veziroglu, T. N., Eds.; Academic Press: London, 2011; pp 89−185.